Electron-Transfer Reactions of Ruthenium Trisbipyridyl–Viologen Donor–Acceptor Molecules: Comparison of the Distance Dependence of Electron-Transfer Rates in the Normal and Marcus Inverted Regions

Edward H. Yonemoto,† Geoffrey B. Saupe,† Russell H. Schmehl,§ Stefan M. Hubig,‡ Richard L. Riley,† Brent L. Iverson,† and Thomas E. Mallouk*,†

Contribution from the Department of Chemistry and Biochemistry and Center for Fast Kinetics Research, University of Texas at Austin, Austin, Texas 78712, and Department of Chemistry, Tulane University, New Orleans, Louisiana 70118

Received June 29, 1993

Abstract: The rates of photoinduced forward and thermal back electron transfer (ET) in a series of donor–acceptor molecules $(2,2'\text{-bipyridine})_2\text{Ru}(4\text{-CH}_3\text{-}2,2'\text{-bipyridine-}4')(\text{CH}_2)_n(4,4'\text{-bipyridinium-CH}_3)^{4+}$ ($n = 1$–5, 7, 8) were studied by flash photolysis/transient absorbance techniques. The rate of intramolecular forward ET (MLCT quenching) in acetonitrile varies exponentially with the number of carbon atoms in the spacer chain up to $n = 5$ and is roughly constant for $n = 5$, 7, 8, consistent with a predominantly "through bond" electron transfer pathway for short chains and a "through solvent" pathway for longer chains. Encapsulation of the spacer chain by β-cyclodextrin molecules slows the rate of forward ET for $n = 7$, 8, consistent with a "through bond" ET pathway. The rate of back ET, which occurs in the Marcus inverted region, also varies exponentially with n, but more weakly than the forward ET rates. Apparent β values (defined by $k_{ET} = A \exp(-\beta r_{DA})$, where r_{DA} is the donor–acceptor distance) are 1.38 and 0.66 Å^{-1} for forward and back ET, respectively. However, correction of k_{ET} for the distance dependence of the solvent reorganization energy gives similar values (1.0–1.2 Å^{-1}) of β for the two ET reactions. In this case, β describes the distance dependence of $|V|^2$ (V = electronic coupling matrix element) rather than that of k_{ET}.

Electron transfer (ET) reactions play a central role in biological processes such as photosynthesis and respiration and also lie at the heart of many important chemical processes. Although several parameters (the nature and orientation of the reactants, the intervening medium, the free energy change for ET) affect the rates of these reactions, in general the distance between electron donor and acceptor is the most important factor,[1] because of the approximately exponential decrease of ET rates with increasing distance.[2,3]

Very significant experimental effort has been directed toward understanding the distance dependence of ET rates. In general these experimental systems have eliminated the problem of variable distance inherent in intermolecular solution-phase ET by covalently linking the electron donor and acceptor or by freezing their motion in a viscous glass or polymer.[4-12] In all these cases the question of the distance dependence also involves the nature of the spacer, the solvent, and the energetics of the ET reaction. The rate constant (k_{ET}) for nonadiabatic ET reactions, in which electronic coupling between the reactant and product potential energy surfaces is weak, can be described by eq 1. Here V is the

$$k_{ET} = \frac{2\pi}{\hbar}|V|^2\text{FCWD} \qquad (1)$$

electronic coupling matrix element and FCWD is the Franck–Condon weighted density of states.[13] Because V depends on the spatial overlap of donor and acceptor orbitals, it is strongly distance-dependent; it is also sensitive to the nature of the

† Department of Chemistry and Biochemistry, University of Texas at Austin.
‡ Center for Fast Kinetics Research, University of Texas at Austin.
§ Tulane University.
* To whom correspondence should be addressed. Current address: Department of Chemistry, Pennsylvania State University, University Park, PA 16802.
⊕ Abstract published in *Advance ACS Abstracts,* May 1, 1994.

(1) Moser, C. C.; Keske, J. M.; Warncke, K; Farid, R. S.; Dutton, L. P. *Nature* **1992**, *355*, 796.
(2) Closs, G. L.; Miller, J. R. *Science* **1988**, *240*, 440.
(3) (a) Newton, M. D.; Sutin, N. *Annu. Rev. Phys. Chem.* **1984**, *35*, 437. (b) Guarr, T.; McLendon, G. *Coord. Chem. Rev.* **1985**, *68*, 1. (c) Hush, N. S. *Coord. Chem. Rev.* **1985**, *64*, 135. (d) Sutin, N. *Progr. Inorg. Chem.* **1983**, *30*, 441. (e) Marcus, R. A.; Sutin, N. *Biochim. Biophys. Acta* **1985**, *811*, 265.
(4) (a) Miller, J. R.; Beitz, J. V.; Huddleston, R. K. *J. Am. Chem. Soc.* **1984**, *106*, 5057. (b) Beitz, J. V.; Miller, J. R. *J. Chem. Phys.* **1979**, *71*, 4579. (c) Miller, J. R. *Science* **1975**, *189*, 221. (d) Closs, G. L.; Johnson, M. D.; Miller, J. R.; Piotrowiak, P. *J. Am. Chem. Soc.* **1989**, *111*, 3751.
(5) (a) Hush, N. S.; Paddon-Row, M. N.; Cotsaris, E.; Oevering, H.; Verhoeven, J. W.; Heppener, M. *Chem. Phys. Lett.* **1985**, *117*, 8. (b) Verhoeven, J. W.; Paddon-Row, M. N.; Hush, N. S.; Oevering, H.; Heppener, M. *Pure Appl. Chem.* **1986**, *58*, 1285. (c) Oevering, H.; Paddon-Row, M. N.; Heppener, M.; Oliver, A. M.; Cotsaris, E.; Verhoeven, J. W.; Hush, N. S. *J. Am. Chem. Soc.* **1987**, *109*, 3258. (d) Oevering, H.; Verhoeven, J. W.; Paddon-Row, M. N.; Cotsaris, E.; Hush, N. S. *Chem. Phys. Lett.* **1988**, *150*, 179. (e) Paddon-Row, M. N.; Verhoeven, J. W. *New J. Chem.* **1991**, *15*, 107. (f) Jordan, K. D.; Paddon-Row, M. N. *Chem. Rev.* **1992**, *92*, 395.
(6) Larrson, S. *J. Am. Chem. Soc.* **1981**, *103*, 4034.
(7) (a) McGuire, M.; McLendon, G. *J. Phys. Chem.* **1986**, *90*, 2549. (b) Heiler, D.; McLendon, G.; Rogalskyj, P. *J. Am. Chem. Soc.* **1987**, *109*, 7540. (c) Conklin, K. T.; McLendon, G. *J. Am. Chem. Soc.* **1988**, *110*, 3345. (d) McLendon, G. *Acc. Chem. Res.* **1988**, *21*, 160. (e) Helms, A.; Heiler, D.; McLendon, G. *J. Am. Chem. Soc.* **1991**, *113*, 4325.
(8) (a) Schmidt, J. A.; McIntosh, A. R.; Weedon, A. C.; Bolton, J. R.; Connolly, J. S.; Hurley, J. K.; Wasielewski, M. R. *J. Am. Chem. Soc.* **1988**, *110*, 1733. (b) Wasielewski, M. R.; Niemczyk, M. P. *ACS Symp. Ser.* **1986**, *321*, 154. (c) Hofstra, U.; Schaafsma, T. J.; Sanders, G. M.; Van Dijk, M.; Van der Plas, H. C.; Johnson, D. G.; Wasielewski, M. R. *Chem. Phys. Lett.* **1988**, *151*, 169. (d) Wasielewski, M. R.; Johnson, D. G.; Svec, W. A.; Kersey, K. M.; Minsek, D. W. *J. Am. Chem. Soc.* **1988**, *110*, 7219. (e) Wasielewski, M.; Niemczyk, M. P.; Johnson, D. G.; Svec, W. A.; Minsek, D. W. *Tetrahedron* **1989**, *45*, 4785.
(9) (a) Heitele, H.; Michel-Beyerle, M. E. *J. Am. Chem. Soc.* **1985**, *107*, 8286. (b) Finckh, P.; Heitele, H.; Volk, M.; Michel-Beyerle, M. E. *J. Phys. Chem.* **1988**, *92*, 6584. (c) Finckh, P.; Heitele, H.; Michel-Beyerle, M. E. *Chem. Phys.* **1989**, *138*, 1. (d) Heitele, H.; Poellinger, F.; Weeren, S.; Michel-Beyerle, M. E. *Chem. Phys. Lett.* **1990**, *168*, 598.
(10) Ryu, C. K.; Wang, R.; Schmehl, R. H.; Ferrere, S.; Ludwikow, M.; Merkert, J. W.; Headford, C. L.; Elliott, C. M. *J. Am. Chem. Soc.* **1992**, *114*, 430.
(11) (a) Fox, L. S.; Kozik, M.; Winkler, J. R.; Gray, H. B. *Science* **1990**, *247*, 1069. (b) Gray, H. B; Malmström, B. G. *Biochem.* **1989**, *28*, 7499. (c) Bowler, B. E.; Raphael, A. L.; Gray, H. B. *Progr. Inorg. Chem.* **1990**, *38*, 259.
(12) For related electrochemical measurements see: (a) Li, T. T.-T.; Weaver, M. J. *J. Am. Chem. Soc.* **1984**, *106*, 6108. (b) Miller, C.; Cuendet, P.; Grätzel, M. *J. Phys. Chem.* **1991**, *95*, 877. (c) Becka, A. M.; Miller, C. J. *J. Phys. Chem.* **1992**, *96*, 2657. (d) Finklea, H. O.; Hanshew, D. D. *J. Am. Chem. Soc.* **1992**, *114*, 3173. (e) Chidsey, C. E. D. *Science* **1991**, *251*, 919. (f) Chidsey, C. E. D.; Bertozzi, C. R.; Putvinski, T. M.; Mujsce, A. M. *J. Am. Chem. Soc.* **1990**, *112*, 4301.

0002-7863/94/1516-4786$04.50/0

Scheme 1. Photoinduced Electron Transfer in a 4-Molecule Photosynthetic Assembly[a]

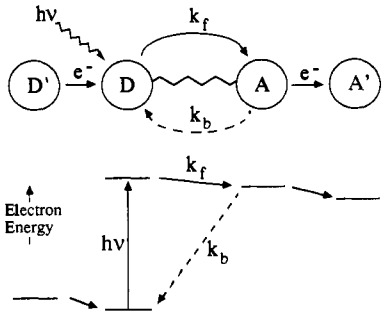

[a] Forward and reverse ET reactions within the D–A molecule are, respectively, in the Marcus normal and inverted rate regions.

intervening medium. Electronic coupling of the donor and acceptor involves superexchange through orbitals of the spacer,[4b] as evidenced by the fact that most measurements give β values in the neighborhood of 1 Å^{-1}. The damping factor β, defined by eq 2 in which r_{DA} is the

$$|V|^2 = |V_o|^2 \exp(-\beta r_{DA}) \qquad (2)$$

donor–acceptor distance, is predicted to be much larger (ca. 2.8 Å^{-1}) if a simple "through space" electron tunneling mechanism were operative.[14]

The FCWD term in eq 1 contains the dependence of k_{ET} on the free energy change, $\Delta G°_{ET}$, as well as the solvent and reactant "inner sphere" reorganization energies, λ_S and λ_V. Because λ_S varies with distance, both $\Delta G°_{ET}$ and λ_S enter into the overall expression for the distance dependence of k_{ET}. Theoretical calculations of k_{ET} as a function of both $\Delta G°_{ET}$ and distance show that while ET rates should be strongly distance-dependent at low driving force (in the Marcus normal region), at high driving force (in the inverted region, where k_{ET} decreases with decreasing $\Delta G°_{ET}$), the rate should depend very weakly on distance.[15] These considerations are very important in the design of artificial photosynthetic systems in which a light-absorbing donor–acceptor molecule initiates the charge-separation process. Such a molecule in general will lie at the center of an array of donors and acceptors, as shown in Scheme 1. The rate of electron transfer from D′ to D$^+$ or from A$^-$ to A′ must compete favorably with the back ET reaction, A$^-$ to D$^+$. In general all the forward ET reactions, including that from photoexcited D to A, will be weakly exoergic and lie in the normal region. Back ET will be highly exoergic and should in fact occur in the Marcus inverted region if $-\Delta G° > \lambda_S$. Under these circumstances the correct choice of intermolecular distances is essential to the efficiency of light-driven electron transfer from D′ to A′.

Scheme 1 describes the photosynthetic reaction center as well as synthetic triads, tetrads, and pentads designed for artificial photosynthesis.[16] It also applies to a number of recently described microheterogeneous systems containing photosensitizers in conjunction with molecular donors and acceptors.[17] Surprisingly, there are no systematic measurements of the distance dependence of ET rates in the Marcus inverted region, despite the relevance of these rates to Scheme 1. A direct comparison of photochemical forward and thermal back ET rates in D–A systems as a function of spacer length is also interesting from a fundamental point of view, because it provides a measure of "electron" vs "hole" superexchange in the same molecule. Previous experiments, carried out by pulse radiolysis, have shown nearly identical distance dependences for electron (radical anion to neutral) and hole (radical cation to neutral) transfers at low driving force.[18] Recent *ab initio* calculations suggest, however, that $|V|^2$ should be somewhat more strongly distance-dependent for radical anions than for radical cations;[19] moreover, the description of superexchange in terms of pure "electron" or "hole" pathways appears to be inappropriate for all but the shortest spacers, because a multitude of pathways contribute to V.[19,20]

In this paper we report the rates of photoinduced forward and thermal back ET reactions in a series of ruthenium trisbipyridyl–methylviologen donor–acceptor molecules covalently linked by flexible aliphatic $(CH_2)_n$, n = 1–5, 7, 8 spacers. Previous work has established that, for short spacer chains (n = 1, 2), these reactions lie respectively in the normal and inverted rate regions.[21] Under conditions where the spacer chain is held in an extended conformation, a linear dependence of ln k_{ET} on distance is found for the entire series. As expected, the back ET rates are much more weakly dependent on distance than the forward rates. The difference can however be accounted for quantitatively by the distance dependence of λ_S, and correcting for this factor we find that the distance dependence of $|V|^2$ is very similar for the forward and back ET reactions.

Experimental Section

Materials. HPLC grade tetrahydrofuran (THF) was opened immediately prior to its use in the synthesis of modified 4,4′-dimethyl-2,2′-bipyridine ligands. The 4,4′-dimethyl-2,2′-bypyridine was obtained

(13) (a) Marcus, R. A. *J. Chem. Phys.* **1956**, *24*, 966. (b) Hush, H. S. *Trans. Faraday. Soc.* **1961**, *57*, 577. (c) Levich, V. O. *Adv. Electrochem. Electrochem. Eng.* **1966**, *4*, 249. (d) Dogonadze, R. R. In *Reactions of Molecules at Electrodes*; Hush, N. S., Ed.; Wiley-Interscience: New York, 1971. (e) Kestner, N. R.; Jortner, J.; Logan, J. *J. Phys. Chem.* **1974**, *78*, 2148. (f) Ulstrup, J.; Jortner, J. *J. Chem. Phys.* **1975**, *63*, 4358. (g) Jortner, J. *J. Chem. Phys.* **1976**, *64*, 4860. (h) Newton, M. D. *Int. J. Quantum Chem., Quantum Chem. Symp.* **1980**, *14*, 363. (i) Brunschwig, B. S.; Logan, J.; Newton, M.; Sutin, N. *J. Am. Chem. Soc.* **1980**, *102*, 5798.

(14) Gamow, G. *Z. Phys.* **1928**, *58*, 204.

(15) Brunschwig, B.; Ehrenson, S.; Sutin, N. *J. Am. Chem. Soc.* **1984**, *106*, 6858.

(16) (a) Gust, D.; Moore, T. A.; Moore, A. L.; Lee, S.-J.; Bittersmann, E.; Luttrull, D. K.; Rehms, A. A.; DeGraziano, J. M.; Ma, X. C.; Gao, F.; Belford, R. E.; Trier, T. T. *Science* **1990**, *248*, 199. (b) Gust, D.; Moore, T. A. *Science* **1989**, *244*, 35, and references therein. (c) Wasielewski, M. R.; Niemczyk, M. P.; Svec, W. A.; Pewitt, E. B. *J. Am. Chem. Soc.* **1985**, *107*, 5562. (d) Danielson, E.; Elliott, C. M.; Merkert, J. W.; Meyer, T. J. *J. Am. Chem. Soc.* **1987**, *109*, 2519.

(17) (a) Slama-Schwok, A.; Avnir, D.; Ottolenghi, M. *J. Phys. Chem.* **1989**, *93*, 7544. (b) Slama-Schwok, A.; Avnir, D.; Ottolenghi, M. *J. Am. Chem. Soc.* **1991**, *113*, 3984. (c) Slama-Schwok, A.; Avnir, D.; Ottolenghi, M. *Nature* **1992**, *355*, 240. (d) Sassoon, R. E.; Gershuni, S.; Rabani, J. *J. Phys. Chem.* **1992**, *96*, 4692. (e) Rabani, J. in *Photoinduced Electron Transfer*, Fox, M. A.; Chanon, M., Eds., Elsevier: Amsterdam, 1988, Part B, pp 642–696. (f) Sassoon, R. E. *J. Am. Chem. Soc.* **1985**, *107*, 6133. (g) Rabani, J.; Sassoon, R. E. *J. Photochem.* **1985**, *29*, 7. (e) Morishima, Y.; Itoh, Y.; Nozakura, S.-I.; Ohno, T.; Kato, S. *Macromolecules* **1984**, *17*, 2264. (h) Hurst, J. K. in *Kinetics and Catalysis in Microheterogeneous Systems*, Grätzel, M.; Kalyanasundaram, K., Eds., Marcel Dekker: New York, 1991, pp 183–226. (i) Thompson, D. H. P.; Barrette, W. C.; Hurst, J. K. *J. Am. Chem. Soc.* **1987**, *109*, 2003. (j) Patterson, B. C; Thompson, D. H.; Hurst, J. K. *J. Am. Chem. Soc.* **1988**, *110*, 3656. (k) Hurst, J. K.; Thompson, D. H. P; Connolly, J. S. *J. Am. Chem. Soc.* **1987**, *109*, 507. (l) Vermuelen, L. A.; Thompson, M. E. *Nature* **1992**, *358*, 656. (m) Ungashe, S. B.; Wilson, W. L.; Katz, H. E.; Scheller, G. R.; Putvinski, T. M. *J. Am. Chem. Soc.* **1992**, *114*, 8717. (n) Nakato, T.; Kazuyuki, K.; Kato, C. *Chem. Mater.* **1992**, *4*, 128. (o) Nakato, T.; Kuroda, K; Kato, C. *J. Chem. Soc. Chem. Commun.* **1989**, 1114. (p) Miyata, H.; Sugahara, Y.; Kuroda, K.; Kato, C. *J. Chem. Soc., Faraday Trans. 1* **1988**, *84*, 2677. (q) Faulkner, L. R.; Suib, S. L.; Renschler, C. L.; Green, J. M.; Bross, P. R. In *Chemistry in Energy Production*, Wymer, R. G., Keller, O. L., Eds.; John Wiley and Sons: New York, 1982; pp 99–114. (r) Persaud, L.; Bard, A. J.; Campion, A.; Fox, M. A.; Mallouk, T. E.; Webber, S. E.; White, J. M. *J. Am. Chem. Soc.* **1987**, *109*, 7309. (s) Krueger, J. S.; Mayer, J. E.; Mallouk, T. E. *J. Am. Chem. Soc.* **1988**, *110*, 8232. (t) Kim, Y. I.; Salim, S.; Huq, M. J.; Mallouk, T. E. *J. Am. Chem. Soc.* **1991**, *113*, 9561. (u) Kim, Y. I.; Riley, R. L.; Huq, M. J.; Salim, S.; Le, A. N.; Mallouk, T. E. in *Synthesis/Characterization and Novel Applications of Molecular Sieve Materials*; Bedard, R. L., Ed.; Materials Research Society: Pittsburgh, PA, 1991; pp 145–156. (v) Incavo, J. A.; Dutta, P. K. *J. Phys. Chem.* **1990**, *94*, 3075. (w) Dutta, P. K.; Turbeville, W. J. Phys. Chem. **1992**, *96*, 5024. (x) Dutta, P. K.; Turbeville, W. *J. Phys. Chem.* **1992**, *96*, 9410. (y) Borja, M; Dutta, P. K. *Nature* **1993**, *362*, 43. (z) Sankaraman, S.; Yoon, K. B.; Yake, T.; Kochi, J. *J. Am. Chem. Soc.* **1991**, *113*, 1419.

(18) Johnson, M. D.; Miller, J. R.; Green, N. S.; Closs, G. L. *J. Phys. Chem.* **1989**, *93*, 1173.

(19) Liang, C.; Newton, M. D. *J. Phys. Chem.* **1993**, *97*, 3199.

(20) Naleway, C. A.; Curtiss, L. A.; Miller, J. R. *J. Phys. Chem.* **1991**, *95*, 8434.

(21) Yonemoto, E. H.; Riley, R. L.; Kim, Y. I.; Atherton, S. J.; Schmehl, R. H.; Mallouk, T.E. *J. Am. Chem. Soc.* **1992**, *114*, 8081.

by barter agreement with Prof. C. Michael Elliott and was recrystallized from ethyl acetate before use. Acetonitrile was distilled from boron oxide under nitrogen. β-Cyclodextrin was obtained from Aldrich and used without purification. All other materials were of reagent grade quality and were used as received. Solvents used in transient spectroscopic measurements were spectrochemical grade. [Ru(2,2′-bipyridine)$_2$(4-((1′-methyl-4,4′-bipyridinediium-1-yl)methyl)-4′-methyl-2,2′-bipyridine)]-(PF_6^-)$_4$·2H$_2$O (H1M), [Ru(2,2′-bipyridine)$_2$(4-(2-(1′-methyl-4,4′-bipyridinediium-1-yl)ethyl)-4′-methyl-2,2′-bipyridine)](PF_6^-)$_4$·2H$_2$O (H2M), and [1-methyl-4,4′-bipyridinium](I^-) were synthesized as described previously.[21] Synthetic methods outlined in the literature[22] were used to prepare functionalized 4,4′-dimethyl-2,2′-bipyridine ligands, as described below. CHN elemental analyses were carried out by Atlantic Microlabs, Inc., Northcross, GA.

4-(3-Hydroxypropyl)-4′-methyl-2,2′-bipyridine. In a drybox, lithium diisopropylamide (3.5 g, 0.033 mol) and a stir bar were placed in a 1000-mL, round-bottom flask equipped with a dropping funnel. The flask was cooled in an ice bath, and 50 mL of THF was added dropwise with stirring to yield an orange-brown solution. This was followed by dropwise addition of 4,4′-dimethyl-2,2′-bypyridine (5.0 g, 0.027 mol) in 150 mL of THF, resulting in a dark brown solution, which was allowed to stir for an additional 20 min. Ethylene oxide (1.5 mL, 0.030 mol) was dissolved in 50 mL of THF and added to the dark brown solution, which then became greenish-blue. This solution was stirred for an additional hour whereupon the solution became yellowish-brown. The reaction was then quenched by slow addition of 10 mL of water. The dropping funnel was taken off, the flask was removed from the ice bath, and the reaction mixture was allowed to warm with stirring to room temperature. A concentrated phosphate buffer (100 mL, pH = 7) was added, and then the reaction mixture was extracted with diethyl ether. The ether extracts were dried over magnesium sulfate, and the ether was removed by rotary evaporation, yielding a yellow-brown oil. This oil was dissolved in chloroform, placed on a short silica column, and eluted with ether. The brown impurity remains on the column, and the product elutes as a yellow band. The ether was removed by rotary evaporation leaving a yellow oil as the product: yield 4.8 g, 0.021 mol (78%); ^{1}H NMR ($CDCl_3$) δ —CH_2— 1.9 (quintet), CH_3 2.4 (s), —CH_2— 2.8 (t), —CH_2OH 3.6 (t), aromatic 7.1, 8.2, 8.5.

4-(3-Bromopropyl)-4′-methyl-2,2′-bipyridine. 4-(3-Hydroxypropyl)-4′-methyl-2,2′-bipyridine (1.0 g, 0.0044 mol) was refluxed with 10 mL of HBr/acetic acid (45% w/v) for 24 h and cooled to room temperature. The solution solidified as it cooled, and ice water was added to dissolve the solid. A saturated sodium bicarbonate solution was added slowly to the solution until it ceased to produce carbon dioxide. The solution was then extracted with diethyl ether, and the extracts were dried over magnesium sulfate. The ether was evaporated under vacuum at room temperature yielding a yellow-brown oil. The yellow-brown oil was dissolved in chloroform and placed on a short silica column and eluted with ether. The brown impurity remains on the column and the product elutes as a yellow band. The ether was evaporated under vacuum leaving a yellow oil as the product: yield 0.7 g, 0.0024 mol (55%); ^{1}H NMR ($CDCl_3$) δ –CH_2– 2.2 (quintet), CH_3 2.4 (s), –CH_2– 2.8 (t), –CH_2Br 3.4 (t), aromatic 7.1, 8.2, 8.5.

4-(4-Bromobutyl)-4′-methyl-2,2′-bipyridine. Lithium diisopropylamide (3.5 g, 0.033 mol) in 50 mL of THF was reacted with 4,4′-dimethyl-2,2′-bypyridine (5.0 g, 0.027 mol) in 150 mL of THF as described above for the preparation of 4-(3-hydroxypropyl)-4′-methyl-2,2′-bipyridine. 1,3-Dibromopropane (5 mL, 0.049 mol) was dissolved in 50 mL of THF and added at once to the dark brown solution, which became dark blue. The solution was stirred at ice temperature for an additional hour whereupon its color became pale yellow. Slow addition of the dibromoalkane yields products where two 4,4′-dimethyl-2,2′-bipyridine molecules are linked together. The reaction was quenched by slow addition of 10 mL of water. The dropping funnel was removed, the flask was removed from the ice bath, and the reaction mixture was allowed to warm to room temperature. About 100 mL of a concentrated phosphate buffer (pH = 7) was then added and the reaction mixture was extracted with diethyl ether. The ether extracts were dried over magnesium sulfate, and the ether was removed under vacuum at room temperature. Heating the product was avoided in order to prevent the self-quaternization reaction. The resulting yellow-brown oil was dissolved in chloroform, placed on a short silica column, and eluted with ether. The brown impurity remains on the column, and the product elutes as a yellow band. The ether was removed under vacuum leaving a yellow oil, which upon standing becomes a waxy solid: yield 7.15 g, 0.023 mol (87%); ^{1}H NMR ($CDCl_3$) δ –CH_2– 1.4 (quintet), –CH_2– 1.9 (quintet), CH_3 2.4 (s), –CH_2– 2.7(t), –CH_2Br 3.4 (t), aromatic 7.1, 8.2, 8.5.

4-(5-Bromopentyl)-4′-methyl-2,2′-bipyridine. The synthesis of this compound was the same as that of 4-(4-bromobutyl)-4′-methyl-2,2′-bipyridine except that 1,4-dibromobutane was used instead of 1,3-dibromopropane: yield 80%; ^{1}H NMR ($CDCl_3$) δ –CH_2– 1.5 (quintet), –CH_2– 1.7 (quintet), –CH_2– 1.9 (quintet), CH_3 2.4 (s), –CH_2– 2.7 (t), –CH_2Br 3.4 (t), aromatic 7.1, 8.2, 8.5.

4-(7-Bromoheptyl)-4′-methyl-2,2′-bipyridine. Again, the synthesis was the same as that of 4-(4-bromobutyl)-4′-methyl-2,2′-bipyridine except that 1,6-dibromohexane was used instead of 1,3-dibromopropane: yield 84%; ^{1}H NMR ($CDCl_3$) δ –CH_2– 1.4 (br), –CH_2– 1.7 (br quintet), –CH_2– 1.8 (quintet), CH_3 2.4 (s), –CH_2– 2.7 (t), –CH_2Br 3.4 (t), aromatic 7.1, 8.2, 8.5.

4-(8-Bromooctyl)-4′-methyl-2,2′-bipyridine. Same as 4-(4-bromobutyl)-4′-methyl-2,2′-bipyridine except that 1,7-dibromoheptane was used instead of 1,3-dibromopropane: yield 79%; ^{1}H NMR ($CDCl_3$) δ –CH_2– 1.4 (br), –CH_2– 1.7 (br quintet), –CH_2– 1.8 (quintet), CH_3 2.4 (s), –CH_2– 2.7 (t), –CH_2Br 3.4 (t), aromatic 7.1, 8.2, 8.5.

[1-(3-(4′-Methyl-2,2′-bipyridin-4-yl)propyl)-1′-methyl-4,4′-bipyridinediium](PF_6^-)$_2$. 4-(3-Bromopropyl)-4′-methyl-2,2′-bipyridine and a slight excess (1.2–1.5 equiv) of [1-methyl-4,4′-bipyridinium](I^-) were refluxed in acetonitrile for 3 days under nitrogen, and the product precipitated as a reddish-brown solid. The solvent was then removed by rotary evaporation, and the solid was dissolved in water. A concentrated aqueous solution of ammonium hexafluorophosphate was then added to precipitate the hexafluorophosphate salt. The product was filtered on a medium frit and washed with water, chloroform, and diethyl ether. The chloroform and ether washings removed any unreacted starting materials (4-(3-bromopropyl)-4′-methyl-2,2′-bipyridine and 4,4′-dimethyl-2,2′-bipyridine). In some instances, it was necessary to redissolve the hexafluorophosphate salt in acetonitrile and reprecipitate the product by dropwise addition with stirring to an aqueous solution of ammonium hexafluorophosphate, in order to remove unreacted excess [1-methyl-4,4′-bipyridinium](PF_6^-). The precipitate was then filtered on a medium frit and washed with water, chloroform, and ether: yield 20%; ^{1}H NMR (CD_3CN) δ –CH_2–, CH_3 2.4 (quintet + s), –CH_2– 2.9 (t), N^+CH_3 4.4 (s), N^+CH_2– 4.7 (t), aromatic 7.2–8.9.

[1-(4-(4′-Methyl-2,2′-bipyridin-4-yl)butyl)-1′-methyl-4,4′-bipyridinediium](PF_6^-)$_2$. The synthesis was the same as that of [1-(3-(4′-methyl-2,2′-bipyridin-4-yl)propyl)-1′-methyl-4,4′-bipyridinediium]-(PF_6^-)$_2$, except that 4-(4-bromobutyl)-4′-methyl-2,2′-bipyridine was used instead of 4-(3-bromopropyl)-4′-methyl-2,2′-bipyridine: yield 31%; ^{1}H NMR (CD_3CN) δ –CH_2– 1.8 (quintet), –CH_2– 2.1 (quintet), CH_3 2.4 (s), –CH_2– 2.8 (t), N^+CH_3 4.4 (s), N^+CH_2– 4.7 (t), aromatic 7.2–8.9.

[1-(5-(4′-Methyl-2,2′-bipyridin-4-yl)pentyl)-1′-methyl-4,4′-bipyridinediium](PF_6^-)$_2$. Again the synthesis was the same as that of [1-(3-(4′-methyl-2,2′-bipyridin-4-yl)propyl)-1′-methyl-4,4′-bipyridinediium]-(PF_6^-)$_2$, except that 4-(5-bromopentyl)-4′-methyl-2,2′-bipyridine was used instead of 4-(3-bromopropyl)-4′-methyl-2,2′-bipyridine: yield 30%; ^{1}H NMR (CD_3CN) δ –CH_2– 1.4 (quintet), –CH_2– 1.7 (quintet), –CH_2–2.1 (quintet), CH_3 2.4 (s), –CH_2– 2.8 (t), N^+CH_3 4.4 (s), N^+CH_2– 4.7 (t), aromatic 7.2–8.9.

[1-(7-(4′-Methyl-2,2′-bipyridin-4-yl)heptyl)-1′-methyl-4,4′-bipyridinediium](PF_6^-)$_2$. Synthesis was the same as that of [1-(3-(4′-methyl-2,2′-bipyridin-4-yl)propyl)-1′-methyl-4,4′-bipyridinediium](PF_6^-)$_2$ except that 4-(7-bromoheptyl)-4′-methyl-2,2′-bipyridine was used instead of 4-(3-bromopropyl)-4′-methyl-2,2′-bipyridine: yield 26%; ^{1}H NMR (CD_3CN) δ –CH_2– 1.4 (br), –CH_2– 1.7 (br quintet), –CH_2– 2.0 (br quintet), CH_3 2.4 (s), –CH_2– 2.7 (t), N^+CH_3 4.4 (s), N^+CH_2– 4.6 (t), aromatic 7.2–8.9.

[1-(8-(4′-Methyl-2,2′-bipyridin-4-yl)octyl)-1′-methyl-4,4′-bipyridinediium]-(PF_6^-)$_2$. Synthesis was the same as that of [1-(3-(4′-methyl-2,2′-bipyridin-4-yl)propyl)-1′-methyl-4,4′-bipyridinediium](PF_6^-)$_2$ except that 4-(8-bromooctyl)-4′-methyl-2,2′-bipyridine was used instead of 4-(3-bromopropyl)-4′-methyl-2,2′-bipyridine: yield 24%; ^{1}H NMR (CD_3CN) δ –CH_2– 1.4 (br), –CH_2– 1.7 (br quintet), –CH_2– 2.0 (br quintet), CH_3 2.4 (s), –CH_2– 2.8 (t), N^+CH_3 4.4 (s), N^+CH_2– 4.7 (t), aromatic 7.2–8.9.

[Ru(2,2′-bipyridine)$_2$(4-(3-(1′-methyl-4,4′-bipyridinediium-1-yl)propyl)-4′-methyl-2,2′-bipyridine)](PF_6^-)$_4$·2H$_2$O (H3M), [Ru(2,2′-bipyridine)$_2$-(4-(4-(1′-methyl-4,4′-bipyridinediium-1-yl)butyl)-4′-methyl-2,2′-bipyridine)]-(PF_6^-)$_4$·2H$_2$O (H4M), [Ru(2,2′-bipyridine)$_2$(4-(5-(1′-methyl-4,4′-

(22) (a) Ciana, L. D.; Hamachi, I.; Meyer, T. J. *J. Org. Chem.* **1989**, *54*, 1731. (b) Ghosh, P. K.; Spiro, T. G. *J. Am. Chem. Soc.* **1980**, *102*, 5543. (c) Abruña, H. D.; Breikss, A. I.; Collum, D. B. *Inorg. Chem.* **1985**, *24*, 987.

bipyridinediium-1-yl)pentyl)-4′-methyl-2,2′-bipyridine)](PF$_6^-$)$_4$·2H$_2$O (H5M), [Ru(2,2′-bipyridine)$_2$(4-(7-(1′-methyl-4,4′-bipyridinediium-1-yl)-heptyl)-4′-methyl-2,2′-bipyridine)](PF$_6^-$)$_4$·2H$_2$O (H7M), and [Ru(2,2′-bipyridine)2(4-(8-(1′-methyl-4,4′-bipyridinediium-1-yl)octyl)-4′-methyl-2,2′-bipyridine)](PF$_6^-$)$_4$·2H$_2$O (H8M). The synthesis of these compounds was the same as that of [Ru(2,2′-bipyridine)$_2$(4-(2-(1′-methyl-4,4′-bipyridinediium-1-yl)-ethyl)-4′-methyl-2,2′-bipyridine)](PF$_6^-$)$_4$·2H$_2$O (H2M), described previously.[21] Ru(2,2′-bipyridine)$_2$(CO$_3$)·2H$_2$O[23] was stirred with a slight excess (1.5 equiv) of the appropiate ligand. Typical yields varied between 25 and 45%, the higher yields being obtained with longer reaction times (about 60 h). Column chromatography on silica gel using the same eluent mixture of 5:4:1 (acetonitrile/water/saturated aqueous potassium nitrate) gave similar results for the n = 3–5 compounds. The n = 7,8 compounds were chromatographed once more in order to separate a third greenish-yellow fluorescent band, which smeared behind the product band and eluted with the tail end of the product band. The n = 7,8 compounds were also slightly luminescent on the silica support.

[Ru(2,2′-bipyridine)$_2$(4-(3-(1′-methyl-4,4′-bipyridinediium-1-yl)propyl)-4′-methyl-2,2′-bipyridine)](PF$_6^-$)$_4$·2H$_2$O (H3M): ^{1}H NMR (CD$_3$CN) δ –CH$_2$– 2.4 (quintet), CH$_3$ 2.6 (s), –CH$_2$– 2.9 (t), N$^+$CH$_3$ 4.4 (s), N$^+$CH$_2$– 4.7 (t), aromatic 7.2–9.0; calc (found) C 38.28 (38.33%), H 3.28 (3.23%), N 7.94 (7.97%).

[Ru(2,2′-bipyridine)$_2$(4-(4-(1′-methyl-4,4′-bipyridinediium-1-yl)butyl)-4′-methyl-2,2′-bipyridine)](PF$_6^-$)$_4$·2H$_2$O (H4M): ^{1}H NMR (CD$_3$CN) δ –CH$_2$– 1.8 (quintet), –CH$_2$– 2.1 (quintet), CH$_3$ 2.6 (s), –CH$_2$– 2.8 (t), N$^+$CH$_3$ 4.4 (s), N$^+$CH$_2$– 4.7 (t), aromatic 7.2–8.9; calc (found) C 38.75 (38.59%), H 3.39 (3.33%), N 7.86 (7.90%).

[Ru(2,2′-bipyridine)$_2$(4-(5-(1′-methyl-4,4′-bipyridinediium-1-yl)pentyl)-4′-methyl-2,2′-bipyridine)](PF$_6^-$)$_4$·2H$_2$O (H5M): ^{1}H NMR (CD$_3$CN) δ –CH$_2$– 1.5 (quintet), –CH$_2$– 1.7 (quintet), –CH$_2$– 2.1 (quintet), CH$_3$ 2.6 (s), –CH$_2$– 2.8 (t), N$^+$CH$_3$ 4.4 (s), N$^+$CH$_2$– 4.7 (t), aromatic 7.2–8.9; calc (found) C 39.21 (39.86%), H 3.50 (3.43%), N 7.78 (7.73%).

[Ru(2,2′-bipyridine)$_2$(4-(7-(1′-methyl-4,4′-bipyridinediium-1-yl)heptyl)-4′-methyl-2,2′-bipyridine)](PF$_6^-$)$_4$·2H$_2$O (H7M): ^{1}H NMR (CD$_3$CN) δ –CH$_2$– 1.4 (broad), –CH$_2$– 1.7(br quintet), –CH$_2$– 2.0 (br quintet), CH$_3$ 2.6 (s), –CH$_2$– 2.7 (t), N$^+$CH$_3$ 4.4 (s), N$^+$CH$_2$– 4.6 (t), aromatic 7.2–8.9; calc (found) C 40.09 (39.91%), H 3.71 (3.65%), N 7.63 (7.72%).

[Ru(2,2′-bipyridine)$_2$(4-(8-(1′-methyl-4,4′-bipyridinediium-1-yl)octyl)-4′-methyl-2,2′-bipyridine)](PF$_6^-$)$_4$·2H$_2$O (H8M): ^{1}H NMR (CD$_3$CN) δ –CH$_2$– 1.4 (br), –CH$_2$– 1.7 (br quintet), –CH$_2$– 2.0 (br quintet), CH$_3$ 2.6 (s), –CH$_2$– 2.8 (t), N$^+$CH$_3$ 4.4 (s), N$^+$CH$_2$– 4.6 (t), aromatic 7.2–8.9; calc (found) C 40.52 (40.58%), H 3.81 (3.77%), N 7.56 (7.61%).

[Ru(2,2′-bipyridine)$_2$(4-(7-hydroxyheptyl)-4′-methyl-2,2′-bipyridine)](PF$_6^-$)$_2$·2H$_2$O (H7OH). Ru(2,2′-bipyridine)$_2$Cl$_2$–2H$_2$O[24] (0.36 g, 6.9 × 10^{-4} mol) was refluxed with 4-(7-bromoheptyl)-4′-methyl-2,2′-bipyridine (0.25 g, 7.2 × 10^{-4} mol) and 1.5 g of NaCO$_3$ in 40 mL of 1:1 ethanol/water for 10 h. The solvent mixture was removed under reduced pressure, and then the product was eluted on a silica column using an eluent mixture of 5:4:1 (acetonitrile/water/saturated aqueous potassium nitrate). The product eluted as the first luminescent orange-red band, and a brown impurity remained on the top of the column. Excess KNO$_3$ was removed from the product by evaporating the solvent under reduced pressure to give a red slurry of KNO$_3$ crystals and then adding acetone to precipitate the KNO$_3$ completely. A small amount of ethanol was added to help solvate the product. The solvent was removed under reduced pressure leaving the product as the nitrate salt, which was then dissolved in water and precipitated with a concentrated solution of ammonium hexafluorophosphate. The hexafluorophosphate salt was then vacuum-filtered and washed with water and then ether: yield 0.51 g, 5.0 10^{-4} mol (72%); ^{1}H NMR (CD$_3$CN) d –CH$_2$–1.4 (br), –CH$_2$–1.7 (br), CH$_3$ 2.6 (s), –CH$_2$– 2.7 (t), –CH$_2$OH 3.6 (t), aromatic 7.2–8.6; calc (found) C 44.58 (45.17%), H 4.33 (3.94%), N: 8.21 (8.56%).

Transient Spectroscopic Measurements. Picosecond transient absorbance measurements of the n = 1, 2 compounds, and related molecules containing various substituents to alter $\Delta G°_{ET}$, are described in a previous publication.[21] The n = 3, 4 compounds were measured using a picosecond pump-probe system described elsewhere.[25] ET rates in compounds with longer spacers were measured by nanosecond flash photolysis/transient absorbance methods described previously.[26] Unless otherwise noted, all experiments were done at room temperature (23 ± 1 °C). Solutions were prepared with spectrochemical grade solvents, and solutions were deoxygenated by purging with nitrogen.

The n = 3, 4 compounds were excited with the third harmonic (355 nm) of a mode-locked Nd:YAG laser, and the reduced viologen signal was monitored at 615 nm. Irradiation at 355 nm excites the bipyridine π,π^* transition, and the molecule relaxes on a subpicosecond time scale to produce the metal–ligand charge-transfer (MLCT) excited state.[27] Solutions were contained in 5-mm pathlength quartz cuvettes and had a ground-state absorbance of about 1.0 at the excitation wavelength. The transient actinometer used for the n = 3, 4 molecules was the [(Me$_2$-bpy)$_2$Ru]$_2$(bbdb)$^{4+}$ dimer[28] (see below); calculations of the forward and back electron transfer rate constants for the n = 1–4 compounds are also described below.

For the n = 5–8 compounds, 10 mm cuvettes were used, and the solutions had absorbances of ca. 0.1 at the excitation wavelength, 532 nm. In these cases no reduced viologen transient was observable at 400 or 600 nm, and the forward ET rates were measured by observing the decay of the MLCT transient at 360 nm. The transient actinometer for the n = 5–8 samples was Ru(bpy)$_3^{2+}$, and quantum yields were calculated by comparison of the MLCT transient to that of Ru(bpy)$_3^{2+}$ as previously described.[26] Since β-cyclodextrin is soluble in water but not in acetonitrile, the hexafluorophosphate salts of the n = 7, 8 compounds and the model compound Ru(2,2′-bipyridine)$_2$(4-(7-hydroxyheptyl)-4′-methyl-2,2′-bipyridine), H7OH, were ion exchanged to give their water-soluble chloride salts. Kinetic measurements in these cases were carried out in deoxygenated water with and without added β-cyclodextrin.

The temperature dependence of the MLCT decay rates of H7M and H7OH were measured in 20 mM aqueous β-cyclodextrin solutions using the nanosecond flash photolysis apparatus described above for the n = 5–8 compounds. In this case a Polyscience Polytemp constant temperature bath circulated chilled or heated water through a jacketed 5 mm pathlength quartz cuvette, over the temperature range 0–50 °C.

Results and Discussion

Structure of Donor–Acceptor Compounds. In these studies flexible polymethylene spacers, (CH$_2$)$_n$, were used to connect the 4′-position of the 2,2′-bipyridyl ligand coordinated to the Ru atom with the 4′-nitrogen of the viologen moiety. The structure of molecules in this series is shown below. The shorthand designation XnY describes substitution at the 4- and 4′-positions of the 2,2′-bipyridyl ligands not connected to the spacer (X = H, M), the length of the spacer (n), and substitution on the viologen nitrogen not connected to the spacer (Y = M, C). For example, H4M denotes two unsubstituted 2,2′-bipyridine ligands on Ru,

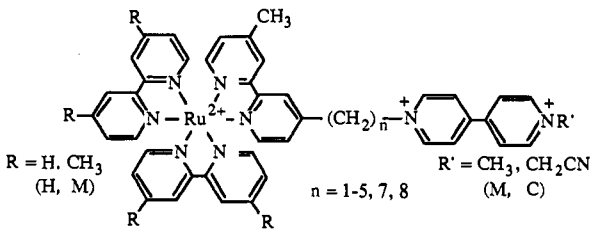

a four-carbon spacer, and a methyl group on the viologen nitrogen. M1C denotes two 4,4′-dimethyl-2,2′-bipyridine ligands on Ru, a one-carbon spacer, and a cyanomethyl group on the viologen. The preparation and ET reactions of the short spacer chain XnY (n = 1, 2) compounds have been reported previously.[21] Variation of Xand Y allows one to observe the dependence of ET rates on $-\Delta G°_{ET}$ and establishes that forward and back ET occur, respectively, in the normal and Marcus inverted regions. In this paper the rates of ET reactions in the HnM series with n = 1–5, 7, and 8, measured at roughly constant $-\Delta G°_{ET}$, are described.

Electrochemistry and Estimation of Reaction Energetics. Cyclic voltammetry for the HnM series in acetonitrile/0.1 M tetrabutylammonium tetrafluoroborate revealed the expected oxidation and reduction waves. The formal potentials listed in Table 1 are the average of the anodic and cathodic peak potentials for each of the reversible waves. Peak potentials for compounds with

(23) Johnson, E. C.; Sullivan, B. P.; Salmon, D. J.; Adeyemi, S. A.; Meyer, T. J. *Inorg. Chem.* **1978**, *17*, 2211.
(24) Lay, P. A.; Sargeson, A. M.; Taube, H. *Inorg. Synth.* **1986**, *24*, 292.
(25) Atherton, S. J.; Hubig, S. M.; Callan, T. J.; Duncanson, J. A.; Snowden, P. T.; Rodgers, M. A. J. *J. Phys. Chem.* **1987**, *91*, 3137.
(26) Mallouk, T. E.; Krueger, J. S.; Mayer, J. E.; Dymond, C. M. G. *Inorg. Chem.* **1989**, *28*, 3507.

Table 1. Formal Potentials[a] of HnM and Related Compounds

compd	$Ru^{3+/2+}$	$V^{2+/+}$	$V^{+/0}$
H1M	+1.295	–0.360	–0.790
H2M	+1.250	–0.400	–0.805
H3M	+1.250	–0.400	–0.795
H4M	+1.220	–0.440	–0.825
H5M	+1.215	–0.440	–0.830
H7M	+1.230	–0.450	–0.865
H7M/β-CD[b]	+0.943	–0.637	
H8M	+1.225	–0.450	–0.860
H8M/β-CD[b]	+0.943	–0.644	
H7OH	+1.230		
MV^{2+}		–0.440	–0.860
$Ru(bpy)_2[(CH_3)_2bpy]^{2+}$	+1.225		

[a] Volts vs saturated calomel electrode (SCE) in CH_3CN/0.1 M $TBA^+BF_4^-$. [b] Volts vs SCE in aqueous 0.1 M KCl/1.0 M HCl/25 mM β-CD.

shorter spacers were shifted to positive potentials relative to those with longer spacers and relative to model compounds H7OH (identical to H7M, except that the methylviologen unit is replaced by an OH group) and methylviologen. With $n \geq 4$ spacers, the formal potentials of the ruthenium-centered oxidation and viologen reductions were essentially the same as those of the model compounds. The excess free energy of the MLCT state (2.08 eV) was estimated from luminescence spectra of the model compound $Ru(bpy)_2[(CH_3)_2bpy]^{2+}$ as described previously.[21]

In order to calculate $\Delta G°_{ET}$ one needs to know, in addition to the formal potentials and excited-state free energy, the change in donor–acceptor electrostatic interaction energy, $\Delta G°_w$, that accompanies electron transfer. This thermodynamic work term was approximated by placing the viologen (+1 or +2) and $Ru(bpy)_3$ (3+ or 2+) charges at their centers of mass, assuming an extended conformation for the polymethylene chain, and using the static dielectric constant ($\epsilon_s = 36.2$) of acetonitrile.[21] Since this term was small (varying between ±0.04 and ±0.02 eV for $n = 1$–8, (–) for forward and (+) for back ET), a more elaborate calculation was deemed unnecessary.

In cases where a change in free energy occurs in bringing the molecule from its lowest energy conformation to the one in which electron transfer occurs, a correction to the free energy of activation, $\Delta G^‡_w$, is required in calculations of k_{ET} from $|V|$, λ_S, λ_V, and $\Delta G°_{ET}$. This additional activation term was previously estimated to be on the order of 0.02 eV for the $n = 2$ compounds, assuming that the most favorable conformation for ET minimizes the through-space donor–acceptor distance and that the lowest energy conformation is the one that minimizes donor–acceptor electrostatic repulsion.[21,27] In the present case, the dependence of ET rates on spacer length (vide infra) strongly suggests that the through space/through solvent pathway is unimportant for $n = 1$–5, and for longer spacers as well when the polymethylene chain is encapsulated by cyclodextrin (CD) molecules. Therefore the $\Delta G^‡_w$ term was not included in calculations of k_{ET}.

Complexation of H7M, H8M, and H7OH by β-Cyclodextrin (β-CD). In order to restrict the donor–acceptor compounds with long spacers to extended polymethylene chain conformations, β-CD was used as a complexing agent. The latter is a torus-shaped oligosaccharide, which has a hydrophilic external and hydrophobic internal surface. The inclusion chemistry of hydrophobic guest molecules in CDs is well documented.[29] In the context of supramolecular electron transfer assemblies, α- and β-CD have been used by Matsuo and co-workers to restrict the motion of donor–spacer–acceptor molecules, in which the electroactive moieties are pyridinium, phenothiazine, and viologen groups.[30] Willner et al. have also used β-CD to complex hydrophobic reduced viologens generated by electron transfer from photoexcited water-soluble porphyrins.[31]

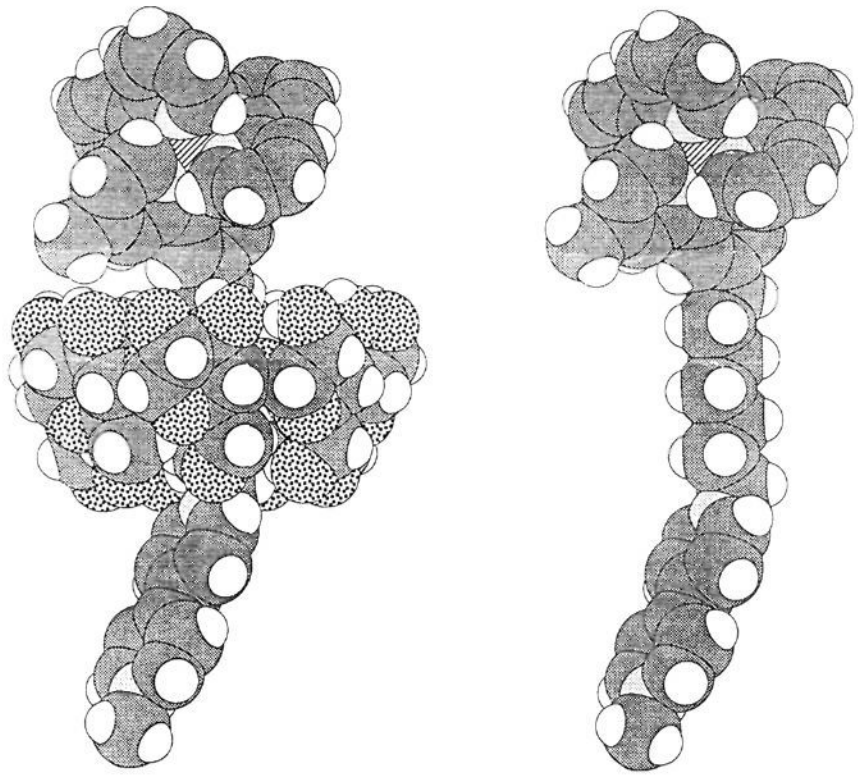

Figure 1. Right: energy-minimized (using Quanta CHARMm, MSI, Inc.) space-filling representation of H7M, shown with the alkyl spacer in the fully extended conformation; left: model of the inclusion complex of H7M in β-CD (cyclodextrin and donor–acceptor molecule minimized separately).

Figure 1 shows energy-minimized space-filling representations of β-CD and H7M, together with a representation of the host–guest complex. It is apparent from this picture that the CD cavity fits neatly over the spacer and should greatly restrict folding motions of the chain. Consistent with this picture we find a dramatic increase in MLCT lifetime (see below) upon addition of 25 mM β-CD to aqueous solutions of H7M and H8M. However, essentially no change is observed in the case of H5M, implying that in this case no complexation occurs. This behavior is consistent with the observations of Matsuo et al.,[30a] who found an association constant of 110 M^{-1} for α-CD with pyridinium-$(CH_2)_8$-pyridinium^{2+}, but no observable complexation with pyridinium-$(CH_2)_6$-pyridinium^{2+}. The inclusion of charged groups such as pyridinium or viologen is sufficiently unfavorable to cause a dramatic decrease in association constant when the length of the spacer chain is smaller than that of the hydrophobic cavity. Importantly, dynamic measurements show that the rate of complex formation/dissociation is slow on the time scale of intramolecular electron transfer.[30]

In the case of the donor–acceptor compounds H7M and H8M, formation constants of β-CD complexes were determined by means of NMR titrations. Figure 2 shows typical spectra, obtained at varying concentrations of β-CD, for H8M in D_2O. The sharp high-field resonances corresponding to protons of the polymethylene spacer gradually broaden and shift. At intermediate β-CD concentrations, resonances for both complexed and uncomplexed H8M are observable, consistent with slow exchange on the NMR time scale. Benesi–Hildebrand plots of the reciprocal intensity change at 1.1 ppm vs reciprocal β-CD concentration gave formation constants of 150 ± 10 and 330 ± 20 M^{-1} for H7M and H8M, respectively. The higher value for H8M reflects a better match between the size of the cyclodextrin cavity and the hydrophobic spacer chain. In the case of H7M, models show (Figure 1) that the fit is rather tight, with the positively charged

(27) (a) Larson, S. L.; Cooley, L. F.; Elliott, C. M.; Kelley, D. F. *J. Am. Chem. Soc.* **1992**, *114*, 9504. (b) Cooley, L. F.; Larson, S. L.; Elliott, C. M.; Kelley, D. F. *J. Phys. Chem.* **1991**, *95*, 10694.

(28) Baba, A. I.; Ensley, H. E.; Schmehl, R. H., submitted to *Inorg. Chem.*

(29) (a) Bender, M. L.; Komiyama, M. *Cyclodextrin Chemistry*; Springer-Verlag: New York, 1978. (b) Saenger, A. Q., *Angew. Chem., Int. Ed. Engl.* **1980**, *19*, 344. (c) Breslow, R. *Science* **1982**, *218*, 532. (d) Tabushi, I. *Acc. Chem. Res.* **1982**, *15*, 66.

(30) (a) Saito, H.; Yonemura, H.; Nakamura, H.; Matsuo, T. *Chem. Lett.* **1990**, 535. (b) Yonemura, H.; Nakamura, H; Matsuo, T. *Chem. Phys. Lett.* **1989**, *155*, 157.

(31) Willner, I.; Adar, E.; Goren, Z.; Steinberger, B. *New J. Chem.* **1987**, *11*, 769.

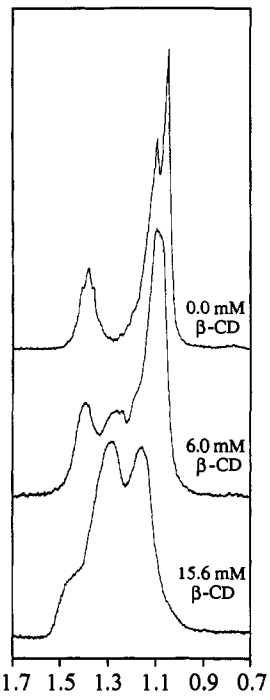

Figure 2. ^{1}H NMR spectra of H8M in D_2O, at varying β-CD concentration. Resonances shown correspond to 10 of the 16 protons in the polymethylene spacer chain.

viologen nitrogen forced partially into the hydrophobic cavity. At concentrations of β-CD used in transient spectroscopic experiments, H7M and H8M were approximately 70% and 90% in the complexed form. The two populations in these cases were reflected by fast and slow excited state decays, as described in the next section.

Determination of Rate Constants from Transient Spectroscopic Data. The sequence of photoinduced electron transfer in these donor–acceptor molecules can be written as

$$\mathrm{MLCT} \xrightarrow{k_f} \mathrm{Ru^{3+}\text{-}MV^{+}} \xrightarrow{k_b} \mathrm{Ru^{2+}\text{-}MV^{2+}} \qquad (3)$$

where the transient concentration of the charge-separated state, Ru^{3+}–MV^+, is given by eq 4.

$$[\mathrm{Ru^{3+}\text{-}MV^{+}}] = \frac{k_f[\mathrm{MLCT}]_0}{k_b - k_f}(e^{-k_f t} - e^{-k_b t}) \qquad (4)$$

In this equation $[MLCT]_0$ represents the concentration of excited states initially generated by the laser flash. For all compounds in the series except $n = 1$, the rate constant of the thermal back reaction, k_b, exceeds that of the forward reaction, k_f. In this case $\exp(-k_b t) \ll \exp(-k_f t)$, and (4) can be approximated by (5),

$$[\mathrm{Ru^{3+}\text{-}MV^{+}}] \approx \frac{k_f[\mathrm{MLCT}]_0}{k_b - k_f}(e^{-k_f t}) \qquad (5)$$

in which the Ru^{3+}–MV^+ state decays by single-exponential kinetics with a rate constant k_f. The value of k_b can nevertheless be determined from (5) if $[MLCT]_0$ is known and $[Ru^{3+}$–$MV^+]$ is extrapolated to time zero. Evaluation of $[MLCT]_0$ is straightforward with visible (532 nm) excitation, using the 360-nm transient absorbance of $Ru(bpy)_3^{2+}$ for actinometry as described previously;[21,26] this procedure was employed for cases where k_f was measured on the nanosecond time scale ($n \geq 5$). For $n < 5$, picosecond excitation at 355 nm was used, and there was insufficient light intensity in the probe continuum to monitor absorbance changes at 360 nm. In this case actinometry was performed with the $[(Me_2bpy)_2Ru]_2(bbdb)^{4+}$ dimer, which has

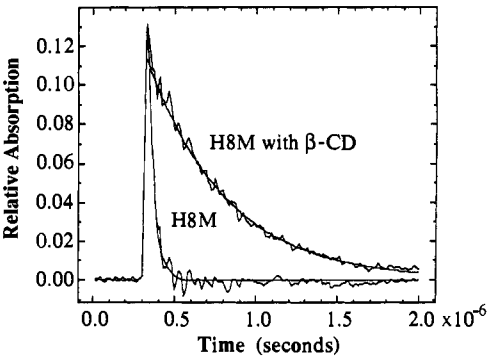

Figure 3. Transient decay of the MLCT excited state of H8M measured in water and in water containing 25 mM β-CD. Line through the data in the latter case corresponds to a fit to the slow component of a biexponential decay.

a long-lived transient absorbance centered at 690 nm.[28] The

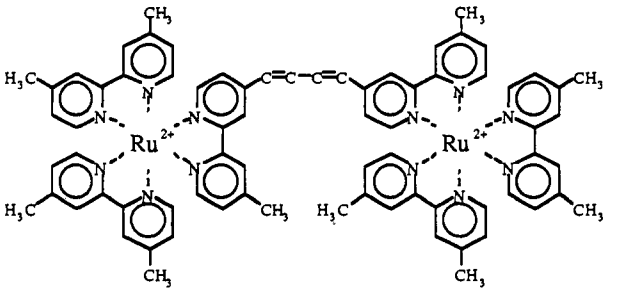

$[(Me_2bpy)_2Ru]_2bbdb^{4+}$

value of k_b was calculated from (6),

$$\frac{k_f}{k_b - k_f} = \left[\frac{\Delta A_{0,615}}{(\Delta\epsilon_{615})(1 - 10^{-A_{355}})}\right]_{\mathrm{sample}} \times \left[\frac{(\Phi_{\mathrm{MLCT}}\Delta\epsilon_{690})(1 - 10^{-A_{355}})}{\Delta A_{0,690}}\right]_{\mathrm{actinometer}} \qquad (6)$$

where the quantity $\Phi_{MLCT}\Delta\epsilon_{690}$ for $[(Me_2bpy)_2Ru]_2(bbdb)^{4+}$ was determined from nanosecond flash photolysis experiments using 355-nm excitation. In this measurement the $Ru(bpy)_3^{2+}$ transient at 360 nm, for which the quantum yield (Φ_{MLCT}) is taken to be unity, was used for calibration.

For the longest spacer chains (H7M and H8M), complexation by β-CD results in MLCT decay rates that are relatively slow. In this case, MLCT decay pathways other than intramolecular electron transfer need to be considered in the calculation of k_f. For this purpose, the model compound H7OH, which lacks the viologen electron acceptor but is still complexed by β-CD, was examined under the same conditions. The forward ET rate constants for H7M and H8M were then calculated from (7):

$$k_f = k_{\mathrm{obs}} - k_{\mathrm{H7OH}/\beta\text{-CD}} \qquad (7)$$

The rates of intramolecular ET in the longer spacer compounds H5M, H7M, and H8M were also measured without β-CD, both in water and in acetonitrile. In all cases, k_f is quite similar in the two solvents; for example, for H8M $k_f = 2.52(3) \times 10^7$ and $2.29(3) \times 10^7$ s^{-1} in acetonitrile and water, respectively. This observation is consistent with expectations of very similar λ_S values for the two solvents[32] and permits direct comparison between them in the following discussion. Figure 3 shows the transient decay of the MLCT excited state of H8M, monitored at 360 nm, following 11-ns laser excitation. In the absence of cyclodextrin, a fast, single exponential decay is found, whereas in the presence of β-CD the decay becomes biexponential. In the latter case the

Table 2. Kinetic Data[a] for Electron-Transfer Reactions of HnM Donor–Acceptor Compounds

compd	ln k_f	ln k_b
H1M	24.8(2)	24.4(2)
H2M	22.79(7)	23.48(5)
H3M	21.4(2)	22.6(2)
H4M	20.3(2)	21.9(2)
H5M	17.99(4)	
H7M	17.66(5)	
H8M	17.0(2)	
H7M/β-CD	14.65(7)[b]	
H8M/β-CD	12.1(4)[b]	
H7OH	14.56(2)[c]	
H7OH/β-CD	14.50(2)[c]	

[a] Rate constants measured in acetonitrile (H1M–H5M) and water (H7M, H8M) at 23 °C. Numbers in parentheses reflect error in the last digit. [b] Slow component of the biphasic decay, electron-transfer rate constant calculated from decay rate constant using eq 7. [c] MLCT decay rate constant.

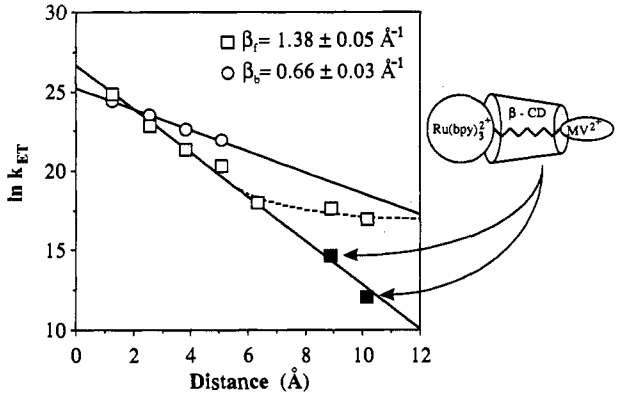

Figure 4. Forward (squares) and back (circles) ET rate constants vs edge-to-edge through-bond distance (calculated as 1.27 Å per CH_2) for HnM in acetonitrile. Error bars lie within the data point boundaries. Filled squares: H7M and H8M in 25 mM β-CD.

decay is dominated by the slower component, consistent with encapsulation of ca. 90% of the H8M molecules by cyclodextrin. Similarly obtained decays of H7M in the presence of β-CD had a larger fast component, consistent with the lower formation constant of the supramolecular complex. Kinetic rate data for forward and back electron transfer in the HnM series are compiled in Table 2.

Distance Dependence of Electron Transfer Rates. Figure 4 summarizes the kinetic data obtained for the series HnM, including rate constants for H1M and H2M reported previously.[21] For $n < 5$, the charge separated state can be observed directly, allowing a calculation of k_b from (6), whereas for $n > 5$, no reduced viologen transient was observable, and only k_f could be determined from transient spectra. Estimated errors in rate constants are smaller than the size of data points shown, except for H8M/β-CD.

Several features of the k_f and k_b plots are noteworthy. First, the forward reaction rates vary exponentially with distance (calculated as bipyridine to viologen edge-to-edge, and assuming a through-bond pathway, 1.27 Å per CH_2) up to $n = 5$. For longer chains, the rates are faster than those defined by the n = 1–5 line and are roughly constant. Complexation by β-CD, however, brings the n = 7, 8 points back onto the line. The rate constant for back ET also varies exponentially with distance; however, in this case the decay is much weaker. Apparent β values, uncorrected for the distance dependence of λ_S, are 1.38 and 0.66 Å^{-1} for forward and back ET, respectively.

The distance dependence of k_{ET} for the forward and back reactions ($n < 5$) supports an ET mechanism involving superexchange through the polymethylene spacer. The fact that ln k_{ET} decays linearly with through-bond distance over this range of spacer length shows that chain conformation has relatively little effect on k_{ET}, since conformational changes are expected to occur on a timescale of 10–100 ps,[33] whereas the ET time scales vary from ca. 10 ps to 10 ns. This point is underscored by the continuation of the linear trend in ln k_f for n = 7, 8 when β-CD is used to hold the spacer chain in an extended conformation. Without β-CD, forward ET rates for $n > 5$ are roughly constant with spacer length. This behavior is consistent with conformational freedom of the longer chains, allowing relatively close through space/through solvent contact of donor and acceptor, and the predominance of that pathway over the slower one through bonds. Similar effects were recently observed by Wagner and co-workers for intramolecular triplet energy transfer in donor–acceptor molecules linked by flexible chains.[34]

Distance Dependence of the Solvent Reorganization Energy. As noted above, the rate constant k_{ET} may be expressed as the product of electronic coupling and Franck–Condon terms. Equation 1 can be expanded to show the explicit dependence of the Franck–Condon term (also called the nuclear factor) on driving force and reorganization energies. In the normal region, the solvent and molecular vibrations can be treated classically, giving (8)

$$k_f = \frac{2|V|^2}{h}\left(\frac{\pi^3}{\lambda k_B T}\right)^{1/2} \exp\left\{\frac{-(\Delta G^\circ + \lambda)^2}{4\lambda k_B T}\right\} \qquad (8)$$

as the expression for k_f.[3e,35] Here λ represents the sum of inner and outer sphere (molecular and solvent) reorganization energies. In the inverted region, the classical description is inadequate and is usually replaced by one in which a single (or average) high vibrational frequency mode of the donor–acceptor molecule is treated quantum mechanically.[4a,13] In the resulting expression for k_b (eq 9),

$$k_b = \frac{2|V|^2}{h}\left(\frac{\pi^3}{\lambda_S k_B T}\right)^{1/2} \sum_{w=0}^{\infty} (e^{-S} S^w / w!) \times \exp\left\{\frac{-(\Delta G^\circ + \lambda_S + wh\nu)^2}{4\lambda_S k_B T}\right\} \qquad (9)$$

the total reorganization energy λ has been replaced by the solvent reorganization energy λ_S. The energy of the vibrational quantum in the high-frequency internal mode is $h\nu$, and S ($=\lambda_V/h\nu$) is a unitless displacement factor for that mode.

In both the normal and inverted regions the Franck–Condon term depends on λ_S, which increases with increasing donor–acceptor separation. The effect of increasing λ_S on k_{ET} is sketched schematically in Figure 5. Equations 8 and 9 predict a parabolic dependence of ln k_{ET} on $-\Delta G^\circ$ in the normal region and an approximately linear dependence deep in the Marcus inverted region. The effect of increasing the donor–acceptor distance is to decrease $|V|$, shifting these curves down, and to increase λ_S, shifting them to the right. At constant driving force, the resultant down-and-to-the-right shift gives rise to a weaker dependence of k_{ET} on distance in the inverted region than in the normal region. It is also apparent from Figure 5 that the extent to which k_b depends on distance is sensitive to $-\Delta G^\circ_{ET}$. At very large driving force, k_b should be invariant with distance, and in fact in certain regimes of distance and $-\Delta G^\circ_{ET}$, k_b has actually been predicted to increase with increasing distance.[15] These considerations led

(32) Brunschwig, B. S.; Ehrenson, S.; Sutin, N. *J. Phys. Chem.* **1986**, *90*, 3657.
(33) (a) Reeves, M. S.; Williams, G. *Adv. Mol. Relaxation Processes* **1975**, *7*, 237. (b) Levy, R. M.; Karplus, M.; McCammon, J. A. *Chem. Phys. Lett.* **1979**, *65*, 4.
(34) (a) Wagner, P. J.; El-Taliawi, G. M. *J. Am. Chem. Soc.* **1992**, *114*, 8325. (b) Wagner, P. J.; Giri, P. B.; Frerking, Jr., H. W.; DeFrancesco, J. *J. Am. Chem. Soc.* **1992**, *114*, 8326.
(35) (a) Brunschwig, B.; Sutin, N. *Comments Inorg. Chem.* **1987**, *6*, 209.

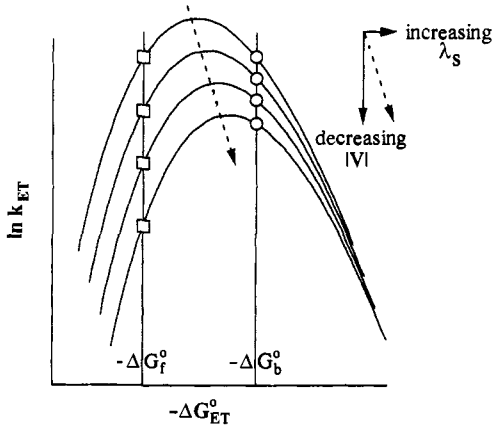

Figure 5. Schematic drawing of ln k_{ET} vs $-\Delta G°$ semiclassical Marcus curves showing the dependence of rate on donor–acceptor distance. Dotted lines represent the resultant direction of curve displacement as $|V|$ decreases and λ_S increases with increasing distance. At constant values of $-\Delta G°$, different distance dependences are observed for ET in the normal (squares) and inverted (circles) regions.

Rau et al. to postulate that the constant rates found for electron transfer between $Ru(R_2bpy)_3^{3+}$ (R = alkyl) and reduced methylviologen, regardless of the size of R, could be attributed to long-distance ET at some optimum distance where k_b is maximized.[36]

In order to extract the distance dependence of $|V|$ from the k_{ET} vs distance data, λ_S must be calculated or measured experimentally. Experimental values of λ_S have been obtained from the energies of optical metal-to-metal charge transfer (MMCT) bands in symmetric bimetallic coordination complexes, and from fits to the free energy dependence of k_{ET} at constant distance.[18,37] In general these measurements are in agreement with claculations of λ_S from models that treat the solvent as a dielectric continuum;[13a,38] however, this agreement is somewhat model- and parameter-dependent,[32] so that $|V|$ vs distance plots derived from theoretical λ_S values should be interpreted with caution.

The simplest approach to calculating λ_S (eq 10)

$$\lambda_S = \left(\frac{e^2}{4\pi\epsilon_0}\right)\left(\frac{1}{2r_D} + \frac{1}{2r_{A_e}} - \frac{1}{R_{DA}}\right)\left(\frac{1}{\epsilon_{op}} - \frac{1}{\epsilon_s}\right) \qquad (10)$$

is the Marcus two-sphere model.[38] This model is most applicable in cases where the donor and acceptor are roughly spherical, and their center-to-center distance (R_{DA}) is large compared to the sum of the sphere radii. In this equation ϵ_{op} and ϵ_s are the high-frequency and static dielectric constants of the solvent, e is the charge transferred, and ϵ_0 is the permittivity of free space. Physically, this model should not apply to donors and acceptors separated by bulky, low dielectric spacers, but in practice it can be used if either the donor or acceptor radius, r_A or r_D, or the quantity $1/r_A + 1/r_D$, is treated as a parameter. Using this approach, Johnson et al. were able to calculate λ_S for a series of donor–acceptor molecules in which the spacers were cyclic and polycyclic aliphatic spacers.[18]

Figure 6 shows fits to eq 8 and 9 of k_{ET} vs $-\Delta G°$ data[21] for the compounds XnY in acetonitrile (X = H, M; n = 1, 2; Y = M, C), using λ_S values calculated from (10). R_{DA} in these calculations was taken as the through-space center-to-center distance, estimated from CPK models. The radius of the roughly spherical $Ru(bpy)_3$ moiety, again from a CPK model, is 6.8 Å. Estimation of the viologen radius is more problematic, since it is shaped more like a halibut than a sphere. An average viologen radius was calculated according to (11),[32]

$$r_A = \frac{1}{2}(d_1 d_2 d_3)^{1/3} \qquad (11)$$

where d_x is the "diameter" along one axis, i.e., the height, width, or length of the viologen molecule. This r_A value, 3.08 Å, gave poor fits of the kinetic data to (8) and (9), as shown in Figure 6, because of serious overestimation of λ_S. Optimal fits were achieved with a larger average viologen radius, 4.8 Å. In the case of complexes encapsulated by β-CD (n = 7,8), the oblong Ru(bpy)3/β-CD complex was approximated as a sphere of radius of 7.96 Å, the latter value being again calculated from dimensions of CPK models and eq 11. λ_S values for the HnM series (n = 1–8), calculated from eq 10, are compared for small and large viologen radii in Table 3.

An approach that is more physically reasonable for donor–acceptor molecules connected by low-dielectric bridges is the

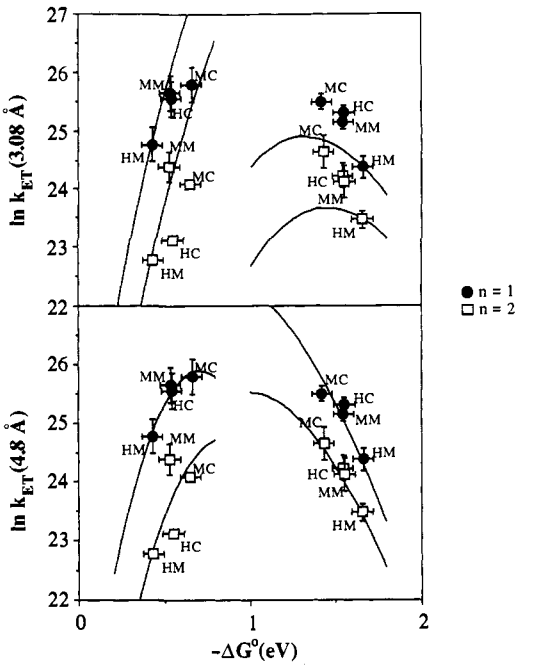

Figure 6. Plots k_{ET} vs $-\Delta G°$ for n = 1 (filled circles) and n = 2 (squares) compounds XnY. Rate data are from ref 21, and solid lines are fits to the two-sphere model. R_{DA} = 9.0 and 10.6 Å for n = 1 and n = 2, respectively. For fits to k_f using (8), λ_v = 0.2 eV. For fits to k_b using (9), $h\nu$ = 0.136 eV (1100 cm^{-1}) and S = 3.0. Top: r_D = 6.8 Å and r_A = 3.08 Å. The k_f fits to (8) used λ_s = 0.9491 eV, $|V|^2 = 3.13 \times 10^{-4}$ eV^2 for n = 1, and λ_s = 1.0767 eV, $|V|^2 = 1.25 \times 10^{-4}$ eV^2 for n = 2. The k_b fits to (9) used λ_s = 0.9491 eV, $|V|^2 = 5.41 \times 10^{-6}$ eV^2, for n = 1, and λ_s = 1.0767 eV, $|V|^2 = 1.63 \times 10^{-6}$ eV^2 for n = 2. Bottom: r_D = 6.8 Å and r_A = 4.8 Å. The k_f fits to (8) used λ_s = 0.5065 eV, $|V|^2 = 8.64 \times 10^{-6}$ eV^2 for n = 1, and λ_s = 0.6341 eV, $|V|^2 = 2.88 \times 10^{-6}$ eV^2 for n = 2. The k_b fits to (9) used λ_s = 0.5065 eV, $|V|^2 = 5.80 \times 10^{-5}$ eV^2 for n = 1 and λ_s = 0.6341 eV, $|V|^2 = 9.21 \times 10^{-6}$ eV^2 for n = 2.

Table 3. Calculated Solvent Reorganization Energies

n^a	R_{DA} (Å)	λ_S (3.08 Å sphere)^b	λ_S (4.8 Å sphere)^b	λ_S (eq 12)
1	9.0	0.9491	0.5065	0.5041
2	10.6	1.0767	0.6341	0.6064
3	11.4	1.1270	0.6845	0.6329
4	12.9	1.2046	0.7621	0.7077
5	13.5	1.2308	0.7883	0.7399
7	15.5	1.2700	0.8101	0.7238
8	16.8	1.3095	0.8496	0.7918

^{a} The calculations are for acetonitrile (ϵ_{op} = 1.80, ϵ_s = 36.7) with n = 1–5, and for water (ϵ_{op} = 1.78, ϵ_s = 78.5) with n = 7, 8. ^{b} Calculated from eq 10.

(36) Rau, H.; Frank, R.; Greiner, G. *J. Phys. Chem.* **1986**, *90*, 2476.
(37) Isied, S. S.; Vassilian, A.; Wishart, J. F.; Creutz, C.; Schwartz, H. A.; Sutin, N. *J. Am. Chem. Soc.* **1988**, *110*, 635.
(38) (a) Marcus, R. A. *J. Chem. Phys.* **1965**, *43*, 58. (b) Marcus, R. A. In *Special Topics in Electrochemistry*; Rock, P. A., Ed.; Elsevier: New York, 1970; p 180.

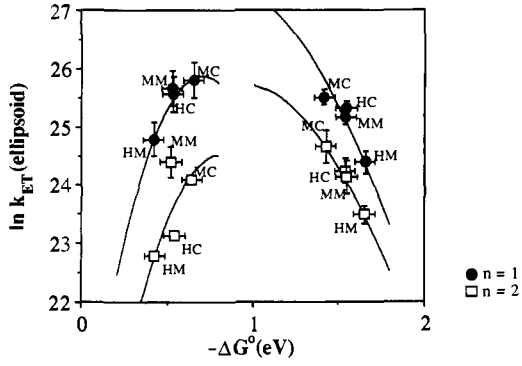

Figure 7. Fits of experimental rate data for XnY (n =1, filled circles; n =2, open squares) to the ellipsoidal model. For fits to k_f using (8), λ_v = 0.2 eV. For fits to k_b using (9), $h\nu$ = 0.136 eV (1100 cm^{-1}) and S = 3.0. The k_f fits to (8) used λ_s = 0.5041 eV, $|V|^2 = 8.500 \times 10^{-6}$ eV^2 for n = 1 and λ_s = 0.6064 eV, $|V|^2 = 2.332 \times 10^{-6}$ eV^2 for n = 2. The k_b fits to (9) used λ_s = 0.5041 eV, $|V|^2 = 5.906 \times 10^{-5}$ eV^2 for n = 1 and with λ_s = 0.6064 eV, $|V|^2 = 1.104 \times 10^{-5}$ eV^2 for n = 2.

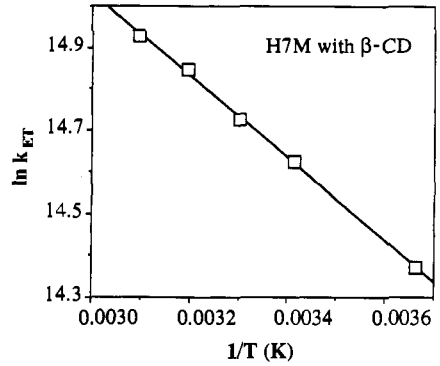

Figure 8. Arrhenius plot showing the temperature dependence of the forward electron-transfer rate for the H7M/β-CD complex in water.

ellipsoidal cavity model originally proposed by Cannon[39] and based on the electrostatic treatment of Kirkwood and Westheimer.[40] This model calculates λ_S according to (12),

$$\lambda_S = \left(\frac{1}{4\pi\epsilon_0}\right)\left(\frac{1}{\epsilon_{op}} - \frac{1}{\epsilon_s}\right)\left[\frac{(\Delta p)^2}{2ab^2}\right]S(\lambda_0) \qquad (12)$$

in which a and b are the radii (semimajor and semiminor axes)of the ellipsoid, Δp is the change in dipole moment ($\Delta p = eR_{DA}$), and the quantity $S(\lambda_0)$ is given by (13),

$$S(\lambda_0) = \sum_{n=0}^{\infty}\frac{1}{2}[1 - (-1)^n]\frac{(2n+1)\lambda_0(\lambda_0^2 - 1)Q_n(\lambda_0)}{P_n(\lambda_0)} \qquad (13)$$

where $(\lambda_0)^2 = a^2/(a^2 - b^2)$, and $P_n(\lambda_0)$ and $Q_n(\lambda_0)$ are the Legendre polynomials of the first and second kinds of degree n. The length of the semimajor axis was taken as half the distance between the van der Waals surfaces of the donor and acceptor, according to (14),

$$a = {}^1/_2(R_{DA} + r_D + r_A) \qquad (14)$$

and the semiminor axis was taken as that of the minimum enclosing-volume-ellipsoid (the "eve" model of Brunschwig et al.[32]). From these values an ellipsoid volume V could be calculated from (15).

$$V = \frac{4}{3}\pi ab^2 \qquad (15)$$

For complexes encapsulated by β-CD (n = 7, 8), the volume was taken to be the sum of the donor–acceptor complex "eve" ellipsoid and the cyclodextrin shell (the latter measured as 830 Å^3 from CPK models), and the value of b was then calculated from (15). This procedure gave values of λ_S, calculated from (12), that were similar to those obtained from the two-sphere model with the large (4.8 Å) viologen radius (Table 3). In the case of the more physically realistic ellipsoidal model, however, the mean acceptor radius (3.08 Å) calculated from (11) was employed, and λ_S was not an adjustable parameter in the fits to the k_{ET} vs $-\Delta G°$ data, shown in Figure 7.

Experimental Determination of λ for the H7M/β-Cyclodextrin Complex. Attempts to make stable cyanomethyl derivatives of the n = 7, 8 compounds, in order to measure the free energy dependence of k_{ET} with long spacer chains, were unsuccessful. An alternative procedure is to extract an experimental activation energy from Arrhenius plots. Figure 8 shows a plot of ln k_{ET} vs $1/T$ for the H7M/β-CD complex in water. Electron-transfer rates were calculated at each temperature from eq 7, by subtracting the MLCT decay rate constant of the model complex H7OH/β-CD. The plot is linear and gives an activation energy of 0.086 eV. Taking $\Delta H^* = -R\,\mathrm{d}(\ln k_f)/\mathrm{d}(1/T)$, the total reorganization energy λ can be calculated from (16–18).[41–43]

$$\frac{(\Delta G° + \lambda)^2}{4\lambda RT} = \Delta H^* - T\Delta S^* \qquad (16)$$

$$\Delta H^{\ddagger} = \Delta H^* - 0.5RT \qquad (17)$$

$$\Delta S^* = \Delta S_{int}{}^* - 0.5\Delta S°(1 + \Delta G°/\lambda) \qquad (18)$$

This calculation requires an estimate of $\Delta S_{int}{}^*$, taken to be +2 eu[42] and measurement of $\Delta S°$ for the forward ET reaction. The latter was obtained by nonisothermal electrochemistry of H7M/β-CD and methylviologen in water. In both cases the standard entropy change for the viologen$^{2+/+}$ couple was found to be –8 eu. Taking the literature value for $\Delta S°$ of the Ru(bpy)$_3{}^{3+/2+}$ couple, +1 eu,[42] and applying a correction of R ln 3 to account for the multiplicity of the MLCT excited state, we obtain $\Delta S°$ = –11 eu for forward ET. This gives a calculated total reorganization energy of 1.27 eV, from which the solvent reorganization energy λ_S is estimated to be 1.07 eV. This value is significantly higher than those predicted from either the two-sphere or ellipsoidal cavity models.

Variation of $|V|^2$ with Donor–Acceptor Distance in the Normal and Inverted Regions. With λ_S values in hand it is possible to extract from the data the dependence of the electronic coupling factor $|V|$ on distance and to obtain values for β (as defined in eq 2) for the forward and back ET reactions. Values of $|V|^2$ were determined from (8) and (9) using the calculated solvent reorganization energies and $\Delta G°$ values for the n = 1–8 series. Figure 9 shows the resulting plots of ln $|V|^2$ vs through-bond distance for the two-sphere and ellipsoidal models. The most striking feature of these plots is the very similar β values (1.0–1.2 Å^{-1}) obtained for back (inverted region) and forward (normal region) ET reactions. The two-sphere model, which predicts a larger distance dependence of λ_S, gives nearly the same β's for the two ET reactions. With the more physically reasonable ellipsoidal cavity model the distance dependence is slightly stronger for the forward ET reaction, as predicted by Liang and Newton,[19] but the difference between the two slopes is small. Conclusions about differences in β's for the forward and back ET reactions must be drawn with caution, because the experimental λ_S value

(39) Cannon, R. D. *Chem. Phys. Lett.* **1977**, *49*, 299.
(40) Kirkwood, J. G.; Westheimer, F. H. *J. Chem. Phys.* **1938**, *6*, 506.
(41) Marcus, R. A.; Sutin, N. *Inorg. Chem.* **1975**, *14*, 213.
(42) Hupp, J. T.; Weaver, M. J. *Inorg. Chem.* **1984**, *23*, 256.
(43) Hupp, J. T.; Weaver, M. J. Inorg. Chem. **1984**, *23*, 3639.

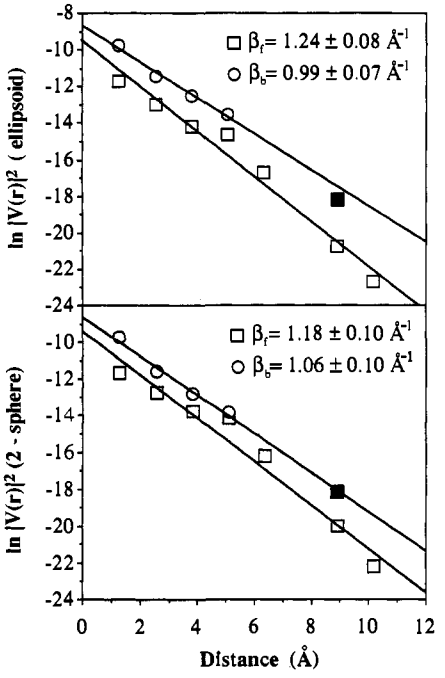

Figure 9. $|V|^2$ vs through-bond edge-to-edge distance (calculated as 1.27 Å/CH_2) for forward (open squares) and back (open circles) ET reactions of HnM. Top: λ_s calculated from the ellipsoidal cavity model. Bottom: λ_s calculated from the two-sphere model using r_A = 4.8 Å. Filled squares show calculated $|V|^2$ for H7M/β-CD using λ_s = 1.07 eV, the value determined from the temperature dependence of k_f.

for H7M/β-CD is larger than that calculated from dielectric continuum models. Larger λ_S values would give smaller and larger β's for the forward and back ET reactions, respectively.

Interestingly, both plots, when extrapolated to zero distance (i.e., edge-to-edge donor–acceptor contact) show stronger electronic coupling for the back than for the forward ET reactions. Assuming that the forward reaction involves predominantly electron superexchange and the back reaction hole superexchange, this difference is at first sight perplexing; the electron in the MLCT excited state exchanges rapidly between the bipyridine ligands, one of which makes close contact with the viologen acceptor, whereas in the charge-separated state the hole resides in a nonbonding orbital of predominantly Ru 4d character, relatively far from the viologen group. In their study of structurally related donor–acceptor complexes, Cooley et al. have made a convincing case that forward electron transfer occurs from the bipyridine ligand connected to the acceptor but that the electron localizes predominantly on the most easily reduced ligands in the MLCT excited state.[44] In the case of the HnM compounds, the remote bipyridine ligands are more easily reduced, by ca. 50 mV, than the 4,4′-dialkylbipyridine ligand in contact with the viologen group. In the work of Cooley et al., this substitution pattern led to a 3–10 fold decrease in k_f, relative to complexes in which all three ligands were 4,4′-dialkylbipyridines. One would predict that this effect would displace the ln $|V|^2$ vs distance curves by 1–2 natural log units for forward ET, but would have little effect on back ET rates. This is in fact the magnitude of the difference in ln $|V|^2$ intercepts found in Figure 9.

(44) Cooley, L. F.; Headford, C. E. L.; Elliott, C. M.; Kelley, D. F. *J. Am. Chem. Soc.* **1988**, *110*, 6673.

Summary and Conclusions

Measurements of ET rates for a series of covalently linked donor–acceptor compounds show that the distance dependence of the forward rates is much stronger than that of the back rates, which are in the Marcus inverted region. This result is of some consequence in the design of donor–acceptor molecules for artificial photosynthesis, because it suggests that shorter spacers should make forward ET more competitive kinetically with (inverted) charge recombination reactions. These considerations apply to polar solvents with large reorganization energies, but not to nonpolar media where both λ_S and its distance dependence are very small.

The difference in distance dependences of k_f and k_b can be accounted for quantitatively by variation of λ_S with distance. Correcting for this effect, β values (1.0 and 1.2 Å^{-1} in the inverted and normal regions, respectively) are consistent with a previous comparison of "electron" and "hole" transfer,[18] and with other measurements of β made with hydrocarbon spacers[4-12] at low driving force. While this result appears to support a recent prediction that ET reactions of radical anions should be more strongly distance dependent than those of radical cations,[19] it should be pointed out that our method of determining $|V|$ rests on somewhat approximate calculations of solvent reorganization energies for longer chains. The activation energy measured for forward electron transfer in the n = 7 case gives a higher λ_S value, which would remove the small difference in β's calculated for normal and inverted region ET. In comparing these results to theoretical predictions of β values, it is also important to recall that β is not an intrinsic property of the spacer but depends on the effective energy gaps connecting it to donor and acceptor orbitals as well as on orientational factors.

Acknowledgment. We thank Dr. Marshall Newton and Prof. Kirk Schanze for helpful discussions, Dr. Donald O'Connor for assisting in the nanosecond flash photolysis experiments, and Andrew Maynard for help with computer programming. This work was supported by the Division of Chemical Sciences, Office of Basic Energy Sciences, Department of Energy, under contract DE-FG05-87ER13789, and by the Welch Foundation. Flash photolysis experiments were carried out at the Center for Fast Kinetics Research (CFKR), University of Texas at Austin. The CFKR is supported jointly by the Biomedical Research Technology Program of the Division of Research Resources of NIH (RR00886) and by the University of Texas at Austin. T.E.M. thanks the Camille and Henry Dreyfus Foundation for support in the form of a Teacher-Scholar Award.

Supplementary Material Available: Kinetic data and exponential fits from which rate constants in Table 2 are derived (2 pages). This material is contained in many libraries on microfiche, immediately follows this article in the microfilm version of the journal, and can be ordered from the ACS; see any current masthead page for ordering information.